Title

Apo-Opsin and Its Dark Constitutive Activity across Retinal Cone Subtypes.

Journal

Current Biology, 30(24)

Authors

Luo, Dong-Gen
Silverman, Daniel
Frederiksen, Rikard
et al.

Publication Date

2020-12-21

DOI

10.1016/j.cub.2020.09.062

Peer reviewed

HHS Public Access

Author manuscript

Curr Biol. Author manuscript; available in PMC 2021 December 21.

Published in final edited form as:

Curr Biol. 2020 December 21; 30(24): 4921–4931.e5. doi:10.1016/j.cub.2020.09.062.

Apo-Opsin and Its Dark Constitutive Activity Across Retinal Cone Subtypes

Dong-Gen Luo[a,b,+,*], **Daniel Silverman**[b,c,1,+], **Rikard Frederiksen**[d], **Rajan Adhikari**[e], **Li-Hui Cao**[a,b], **John E. Oatis**[f], **Masahiro Kono**[f], **M. Carter Cornwall**[e], **King-Wai Yau**[b,g,2,*]

[a]McGovern Institute for Brain Research, Center for Quantitative Biology and Center for Life Sciences, College of Life Sciences, Peking University, Beijing, China

[b]Solomon H. Snyder Department of Neuroscience, Johns Hopkins University School of Medicine, Baltimore, MD 21205, USA

[c]Biochemistry, Cellular and Molecular Biology Graduate Program, Johns Hopkins University School of Medicine, Baltimore, MD 21205, USA

[d]Jules Stein Eye Institute, University of California Los Angeles, Los Angeles, CA 90095, USA

[e]Department of Physiology and Biophysics, Boston University School of Medicine, Boston, MA 02118, USA

[f]Department of Ophthalmology, Medical University of South Carolina, Charleston, SC 29425, USA

[g]Department of Opthalmology, Johns Hopkins University School of Medicine, Baltimore, MD 21205, USA

SUMMARY

Retinal rod and cone photoreceptors mediate vision in dim and bright light, respectively, by transducing absorbed photons into neural electrical signals. Their phototransduction mechanisms are essentially identical. However, one difference is that, whereas a rod visual pigment remains stable in darkness, a cone pigment has some tendency to dissociate spontaneously into apo-opsin and retinal (the chromophore) without isomerization. This cone-pigment property is long

* To whom correspondence may be addressed, at dgluo@pku.edu.cn or kwyau@jhmi.edu.

[1]Present address: Division of Neurobiology, Department of Molecular and Cell Biology, Helen Wills Neuroscience Institute, Howard Hughes Medical Institute, University of California, Berkeley, Berkeley, CA 94720, USA.

[+]Equal contributions to the work

[2]Lead Contact

AUTHOR CONTRIBUTIONS

D.-G.L. did all truncated-cone experiments, physiological characterizations of goldfish cones and background-adaptation experiments in K.-W.Y.'s laboratory nearly a decade ago before his return to China, with subsequent help from L-H.C and D.S. on data analysis. D.S. did some physiological characterizations of goldfish cones, background-adaptation experiments, and studying A_1- and A_2-chromophores on dim-flash sensitivity of L-cones. R.F., R.A. and M.C.C. did the microspectrophotometry and analysis. J.O. and M.K. synthesized the A_2-chromophore. D.-G.L., D.S. and K-W.Y. were behind the final conceptual framework of the project and wrote the paper.

DECLARATION OF INTERESTS

The authors declare no competing interests.

known, but has mostly been overlooked. Importantly, because apo-opsin has weak constitutive activity, it triggers transduction to produce electrical noise even in darkness. Currently, the precise dark apo-opsin contents across cone subtypes are mostly unknown, as are their dark activities. We report here a study of goldfish red (L), green (M) and blue (S) cones, finding with microspectrophotometry widely different apo-opsin percentages in darkness, being ~30% in L cones, ~3% in M cones, and negligible in S cones. L and M cones also had higher dark apo-opsin noise than holo-pigment thermal isomerization activity. As such, given the likely low signal amplification at the pigment-to-transducin/phosphodiesterase phototransduction step especially in L cones, apo-opsin noise may not be easily distinguishable from light responses, thus may affect cone vision near threshold.

IN BRIEF (eToC Blurb)

Cone but not rod pigments can dissociate in darkness into apo-opsin and chromophore without isomerization, but this cone pigment property has been generally overlooked. Luo *et al.* report experiments showing that the dark apo-opsin content especially in L cones is substantial, producing dark noise that may constrain cone photodetection threshold.

Graphical Abstract

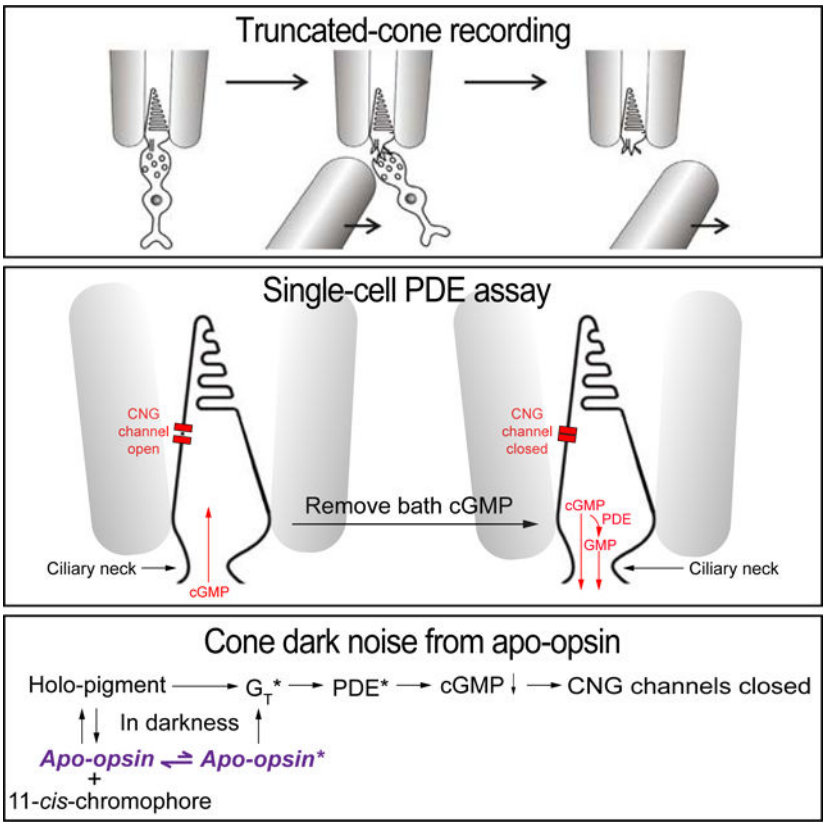

INTRODUCTION

Multiple studies over several past decades have examined the dark noise in retinal rods and cones for understanding phototransduction and correlating noise with the human visual threshold. For rods, whether amphibian or primate, the dark noise arises predominantly from spontaneous activity of rhodopsin ("discrete noise") and from intrinsic activity of the cGMP-phosphodiesterase (PDE) mediating phototransduction ("continuous noise") [1–4]. For cones, an early study on turtle cones reported noise coming from the light-sensitive ion channels [5]. Much later, two studies on salamander L cones reported dark noise dominated by spontaneous pigment isomerization [6,7], whereas another on fish M cones found dark noise mostly from spontaneous PDE activity [8]. For primate cones, the dark noise seems even more complex, with spontaneous isomerization being hardly the main source [9–11]. The reasons for these differences across species remain unclear.

One source of cone noise not given much attention so far is dark constitutive activity of apo-opsin. Cone pigments have some tendency in darkness to dissociate back into apo-opsin and retinal without isomerization [12,13]. Given opsin's weak constitutive ability to activate phototransduction [12,14–17], its presence should trigger noise. Power spectral analysis has been the predominant tool for analyzing photoreceptor noise [1,3–11]. However, this is not always the best way to dissect noise or identify their biological origins, especially to distinguish between closely-related components such as holo-pigment and apo-opsin, which produce overlapping power spectra.

In this work, we focus on the specific question of dark cone apo-opsin content and its constitutive activity. To measure opsin content, we employed primarily microspectrophotometry [18,19]. To characterize dark noise, we employed a truncated-photoreceptor preparation previously developed by us for both rods [20–23] and cones [24] (see also [4,6]), but avoided power spectral analysis. As such, we measured the dark activity of each phototransduction step while preserving the outer segment's native internal compartmentalization. To quantify activity, we assayed PDE activity with a biophysical approach that we previously developed for rods [22].

We studied goldfish cones because they are robust and relatively abundant (~25% of photoreceptors [25]). They comprise L, M, S and UV subtypes [18,26] (cf. salamander cones, with no M cones and unusually sensitive S cones [6,27]). UV cones were omitted because they require special optics.

RESULTS

Qualitative PDE Activity in Darkness

The final effector enzyme in phototransduction is PDE, which hydrolyzes cGMP to close the cyclic-nucleotide-gated (CNG) channels. CNG channels have fast gating (milliseconds) and do not desensitize [28,29], providing a straightforward assay for cytoplasmic cGMP changes and hence PDE activity [22].

To assay PDE activity qualitatively in darkness, we dialyzed a pseudo-intracellular solution (STAR★METHODS) from the bath into a fully dark-adapted cone that was truncated at the inner segment below the ciliary neck and recorded with a suction pipette (Figure 1A, B). Figure 1C shows an L-cone experiment. Initially, with no cGMP or GTP (the latter being required for endogenous cGMP synthesis) present in the dialyzing solution (STAR★METHODS), no dark current was observed. Upon dialyzing in 500-μM cGMP, a large inward current reflecting CNG channels opening appeared. After the CNG current plateaued, 15-μM GTP was added to the dialyzing solution, with the concentration so chosen to permit activation of cone transducin (the G-protein mediating cone phototransduction) but to minimize cGMP synthesis by the cone guanylate cyclase [20,23]. The inward current dramatically decreased almost instantly, reflecting GTP-dependent PDE activity. Upon removing GTP, the inward current returned, which disappeared after cGMP removal. 15-μM GTP without cGMP induced no observable current (see Figure 2 and 3A). Altogether, five L cones gave similar results. The same experiment on M cones yielded a much smaller GTP-induced reduction in CNG current (Figure 1D, n=6). No current-reduction by GTP was observed with S cones (Figure 1E, n=4; see also [6]). Thus, qualitatively, dark GTP-dependent PDE activity was highest in L cones, less in M cones, and undetectable in S cones.

Because L, M and S cones all express the same transducin isoform [30], non-detectable dark GTP-dependent PDE activity in S cones (as in salamander S cones; see [6]) suggests, at least qualitatively, low intrinsic GTP-dependent transducin activity across cone subtypes (see more later). Thus, the dark GTP-dependent PDE activity in L and M cones most likely arose from spontaneous holo-pigment or apo-opsin activity. We next checked the effect of ATP on the GTP-dependent PDE activity. Phosphorylation of the active pigment by its kinase is well-known to initiate active-pigment quenching, thus requiring ATP [23]. Indeed, 1-mM ATP reduced the GTP action (Figure 1F), consistent with at least some spontaneous holo-pigment activity. Constitutive apo-opsin activity may also be quenched by phosphorylation [31,32].

Quantitative Measurement of Dark GTP-Dependent and GTP-Independent PDE Activities

We quantify here the dark GTP-dependent and GTP-independent PDE activities. We first dialyzed 3-mM cGMP (which saturated the CNG current even in face of PDE activity) into the outer segment without GTP and, afterwards, rapidly removed cGMP and measured the rate of cGMP disappearance from the outer segment based on the CNG current decline [21,22]. The dissipation of cGMP resulted from combined diffusion out and hydrolysis by constitutive PDE activity. Assuming cross-sectional homogeneity, cGMP loss by diffusion is a first-order process, being proportional to cGMP concentration with a rate constant γ reflecting cGMP's longitudinal diffusion coefficient [21,22]. cGMP hydrolysis is also a first-order reaction and, when its concentration falls much below PDE's Michaelis constant (K_m) for cGMP, it becomes proportional to cGMP concentration with a rate constant β', where $\beta' = V_{max}/K_m$, with V_{max} being the maximum GTP-independent (intrinsic) enzyme activity. Thus, cGMP concentration should have a final exponential decay with rate ($\beta' + \gamma$). As cGMP falls far below the half-activation constant, $K_{1/2}$, for the cone CNG channel, the current will also decay exponentially with rate $n_H(\beta' + \gamma)$, where n_H is the Hill

coefficient of channel activation by cGMP (~2.4; see [28]). The parameter γ can be isolated by repeating the above procedure with 1-mM IBMX in the dialyzing solution, which inhibits all PDE activity to make $\beta' = 0$ [21,22]. From the difference in CNG-current decline rate with and without IBMX, β' can be evaluated.

Figure 2A shows an L-cone experiment, plotted linearly (top) and semi-logarithmically (bottom). γ was estimated to be 0.016 s^{-1} from the current decay in IBMX (Figure 2A bottom, Trace 3), and ($\beta' + \gamma$) to be 0.088 s^{-1} from the current decay without IBMX (Figure 2A bottom, Trace 1), thus $\beta' = 0.072$ s^{-1}. Collected L-cone experiments gave $\gamma = 0.020 \pm 0.006$ s^{-1} and $\beta' = 0.059 \pm 0.038$ s^{-1} (mean ± SD, n = 10). Figure 2B and 2C show similar M-cone and S-cone experiments, giving collectively $\gamma = 0.017 \pm 0.003$ s^{-1}, $\beta' = 0.050 \pm 0.037$ s^{-1} (n = 7) and $\gamma = 0.025 \pm 0.009$ s^{-1}, $\beta' = 0.059 \pm 0.009$ s^{-1} (n = 3), respectively. By analogy to rods, the GTP-independent PDE activity is interpreted as spontaneous “molecular rocking motion” of the inhibitory PDE γ-subunits on the catalytic PDE α’-subunits [4].

The similar γ values across cone subtypes indicate that longitudinal cGMP diffusions along their outer segments are similar. From $D \sim \gamma L^2$, where D is longitudinal diffusion coefficient and L is outer-segment length (Table S1), we obtain $D \sim 5$ μm^2 s^{-1} for L cones, which is 12-fold lower than for amphibian rods (~60 μm^2 s^{-1}, [21]). This lower D value in cones is expected because their outer-segment intracellular membrane discs are continuous with the plasma membrane, thus introducing a higher tortuosity-factor for longitudinal diffusion. Also, the presence of the narrow ciliary neck between the outer and inner segments (but absent in truncated rod outer segments [21]) might contribute to the lower D value. The similar β' values across L, M and S cones indicate that their dark GTP-independent PDE activities are similar.

In the above experiment, dark GTP-dependent PDE activity, β, could also be measured with 15-μM GTP. From the difference in current decline rate between Trace 1 (without GTP) and Trace 2 (with GTP) in Figure 2A, lower, we obtained $\beta = 0.042$ s^{-1} for the L cone. Corresponding β values could be obtained for M and S cones (Figure 2B and 2C). Collected data gave 0.039 ± 0.019 s^{-1} for L cones (n = 10), 0.004 ± 0.003 s^{-1} (n = 7) for M cones, and below resolution for S cones (n = 3). The undetectable GTP-dependent PDE activity in S cones indicates very low combined pigment thermal isomerization and constitutive apo-opsin activity, as well as negligible uncatalyzed (i.e., intrinsic) GTP-for-GDP exchange on cone transducin. We can generalize the last attribute to L and M cones.

The total dark PDE activity (i.e., GTP-independent and GTP-dependent) corresponds to the basal PDE activity. Our average ($\beta' + \beta$) value of ~0.054 sec^{-1} for M cones is lower than the ~0.24 s^{-1} estimated from intact striped-bass M cones with power spectral analysis [8]. The latter estimate involved biochemical parameters borrowed from amphibian rods [8], so the comparison may not be meaningful.

Equivalent Dark Light for Dark GTP-Dependent PDE Activity

The measured dark GTP-dependent PDE activity, whether due to holo-pigment or apo-opsin, can be converted into an equivalent pigment-isomerization rate as follows. After measuring dark GTP-dependent PDE activity from a truncated cone, we turned on a calibrated steady

light and repeated the measurements. In Figure 3A, left, the first part of experiment on an L cone was identical to that in Figure 2A, giving a cGMP-dissipation rate from combined diffusion and GTP-independent PDE activity of 0.055 s^{-1} (Trace 1). Repeating the measurement with 15-μM GTP yielded an overall cGMP-dissipation rate of 0.091 s^{-1} (Trace 2). Subtracting Trace 1 from Trace 2 gives a dark GTP-dependent PDE activity of 0.036 s^{-1}. Next, with GTP still present, a steady light at L-cone pigment's λ_{max} was delivered at two successively higher intensities and the protocol repeated during each (Traces 3 and 4). Subtracting Trace 1 from Trace 3 or Trace 4 gives light-activated, GTP-dependent PDE activities of 0.051 s^{-1} and 0.065 s^{-1}, respectively. The relation between GTP-dependent PDE activity and steady light intensity (Figure 3A, right) is roughly linear ($R^2 = 0.92$), giving an extrapolated "dark light" of 438 photons μm^{-2} s^{-1}. Collected data from L cones gave an equivalent dark light intensity of 849 ± 290 photons μm^{-2} s^{-1} (n = 10; Figure 3B). Multiplying this value by goldfish L cone's effective collecting area of 1.93 μm^2 (Table S1) gives 1,639 ± 560 equivalent isomerizations s^{-1}. Similar experiments on M cones gave a dark light of 32 ± 15 photons μm^{-2} s^{-1} (n = 7; Figure 3C), or 44 ± 21 equivalent isomerizations s^{-1} for an effective collecting area of 1.37 μm^2 (Table S1). For S cones, the dark GTP-dependent PDE activity was below resolution (Figure 3D).

The somewhat varied estimates in dark light across cells could arise from multiple factors. One was possibly a variation in the percentage of dark apo-opin across cells (see next section). Another was some gradual washout from the outer segment of soluble components in phototransduction or affecting it (see [22] for rods). A third was that ablating the bulk of the cone inner segment to achieve a truncated cell likely affected the known light-dependent translocation of signaling proteins between the outer and inner segments. Nonetheless, this effect may not be large for cones because cone transducin actually does not translocate from outer segment to inner segment even in bright light [33–35]. Cone arrestin is also reportedly distributed across the cone in darkness, although becoming more concentrated in the outer segment in bright light [33,36,37]. The illumination used in our experiments was not very bright or prolonged (Figure 3).

Apo-Opsin Contribution to Dark GTP-Dependent PDE Activity

We would like to separate thermal cone-pigment excitation and constitutive apo-opsin activity. Individual cone-pigment isomerization events are not resolvable in cones owing to their tiny electrical amplitude. As mentioned in Introduction, others resorted to power spectral analysis, but this approach is potentially ambiguous especially in cones (see Discussion). Instead, we used a quantitative physicochemical relation that we previously arrived at for calculating the molecular rate constant of thermal pigment isomerization from the absorption λ_{max} [38–40]. This relation is generally successful in predicting molecular rates for native A_1- and A_2- rod and cone pigments across mammals and amphibians [38]. As such (see Ref. [38] and STAR★METHODS), we estimated the molecular constants of spontaneous isomerization at 23°C to be 5.78×10^{-7} s^{-1} $molecule^{-1}$ for goldfish L-cone pigment (λ_{max} ~ 623 nm), 8.91×10^{-9} s^{-1} $molecule^{-1}$ for M-cone pigment (λ_{max} ~ 537 nm), and 5.30×10^{-12} s^{-1} $molecule^{-1}$ for S-cone pigment (λ_{max} ~ 447 nm). Multiplying by the respective goldfish cone-outer-segment volumes and pigment densities (Table S1), we

obtained spontaneous rates of 167, 3, and 0.002 isomerizations s^{-1} for L, M, and S cones, respectively.

The above expected rates in L and M cones are substantially lower than the equivalent dark light measured by us. We interpret the excess equivalent dark light as being from apo-opsin originating from dark dissociation of holo-pigment. Thus, by subtraction, we obtained the equivalent dark light being attributable to free opsin, namely, ~1,472 equivalent isomerizations s^{-1} for L cones, ~41 equivalent isomerizations s^{-1} for M cones, and unresolvable for S cones.

Next, we correlated the constitutive apo-opsin activity with the amount of apo-opsin present. Previously, based on bleaching adaptation, we roughly estimated that ~10% of in situ salamander L-cone pigment is apo-opsin [12]. However, as noted in [12], this estimate is indirect, and the bleaching-based assay is also especially unsuitable for goldfish cones (see next section), not to mention potential animal-species differences. Accordingly, we quantified apo-opsin content directly with microspectrophotometry in fully-dark-adapted, mechanically isolated single goldfish cones (STAR★METHODS). Figure 4A, B and C show sample measurements from three each of L, M and S cones. Apo-opsin and free chromophore do not absorb strongly in visible light, thus the fractional apo-opsin content can be evaluated from the difference in light absorption by a cone outer segment before (black traces) and after a brief (15-min) exposure to excess 11-*cis*-retinal (A_1-chromophore) in darkness (red, green and blue traces, respectively). The light-absorption increase afterwards indicates apo-opsin in dark-adapted cones being converted into holo-pigment. The 15-min exposure to 11-*cis*-retinal was short enough that any dark replacement of native A_2- by exogenous A_1-chromophore during this duration was negligible [12]. We used A_1-chromophore, although non-native to goldfish, as substitute for two reasons. First, native A_2-chromophore has very limited availability. Second, and more importantly, any increase in the absorption spectrum upon exposure to A_1 chromophore should show a blue-shifted λ_{max} (most dramatic for L cones, progressively less for M- and S-cones; see Figure 4; [12,39,41]), indicating unequivocally *de novo* formation of A_1-visual pigment. A_1-based pigments have an extinction coefficient ~1.4 times that of A_2-based pigments [42], which must be included in apo-opsin calculations ([12], see STAR★METHODS). The post-chromophore-treatment spectrum (post-spectrum) was thus a linear summation of A_1- and A_2-spectra. To quantify apo-opsin, a cone's pre-chromophore-treated spectrum (pre-spectrum) is subtracted from the post-spectrum to give a difference spectrum indicating the amount of A_1-pigment formed. The fractional apo-opsin content in darkness is then given by the ratio between the difference spectrum's peak optical density (after adjustment for the A_2/A_1 extinction-coefficient difference) and the total (adjusted) peak optical density after chromophore exposure.

Figure 4D shows collected data for dark-adapted optical densities and fractional apo-opsin contents of the three cone subtypes, plotted against the time lapse in darkness after mechanical isolation of the cones from the retina and retinal pigment epithelium. Surprisingly but interestingly, there was no sign of any progressive increase in apo-opsin content after cell isolation (see [12] and Discussion). The calculated fractional apo-opsin content was 32.0 ± 6.0% (mean ± S.D., n=14) in dark-adapted L cones, 2.8 ± 4.2% (n=11) in

M cones, and undetectable (n=8) in S cones. Although the S-cone measurements have been pushed to the limit of our optics, this negative finding is consistent with, at least in principle, an undetectable dark GTP-dependent PDE activity in S cones (Figure 1E and Figure 2C).

A fractional apo-opsin level can be converted into apo-opsin molecules based on outer-segment volume and pigment density (3.5 mM; [18,43]), giving (2.02×10^{-13} L) × (3.5 mM × 0.32) × $N_{Avogadro}$ = 1.36×10^{8} apo-opsin molecules in dark-adapted L cones, (1.43×10^{-13} L) × (3.5 mM × 0.028) × $N_{Avogadro}$ = 8.44×10^{6} apo-opsin molecules in dark-adapted M cones, and below detection in dark-adapted S cones. Dividing these numbers into the measured dark constitutive GTP-dependent PDE activity attributable to free opsin, we obtained the molecular rate constant of constitutive cone apo-opsin activity, being 1.08×10^{-5} equivalent isomerizations s^{-1} L-cone opsin^{-1} and 4.86×10^{-6} equivalent isomerizations s^{-1} M-cone opsin^{-1}.

A quantitative breakdown of dark constitutive transduction activity in goldfish cones can now be made. In L cones, ~ [0.059 s^{-1} / (0.059 s^{-1} + 0.039 s^{-1})] = 60% of dark PDE activity came from intrinsic, GTP-independent PDE activity, ~[(167 pigment isomerizations s^{-1} / 1639 total equivalent isomerizations s^{-1}) × 0.039 s^{-1} / (0.059 s^{-1} + 0.039 s^{-1})] = 4% from spontaneous pigment isomerization, and ~[(1,472 equivalent isomerizations s^{-1} / 1639 total isomerizations s^{-1}) × 0.039 s^{-1} / (0.059 s^{-1} + 0.039 s^{-1})] = 36% from constitutive apo-opsin signaling. In M cones, we found that ~[0.050 s^{-1} / (0.050 s^{-1} + 0.004 s^{-1})] = 92.6% of it came from intrinsic PDE activity, ~[(3 pigment isomerizations s^{-1} / 44 equivalent isomerizations s^{-1}) × 0.004 s^{-1} / (0.05 s^{-1} + 0.004 s^{-1})] = 0.5% from spontaneous pigment isomerization, and ~[(41 equivalent isomerizations s^{-1} / 44 total isomerizations s^{-1}) × 0.004 s^{-1} / (0.05 s^{-1} + 0.004 s^{-1})] = 6.9% from constitutive apo-opsin signaling. In S cones, the dark transduction activity was almost entirely from intrinsic, GTP-independent PDE activity (0.059 s^{-1}).

Single-Photon Response, Background Adaptation and Apo-Opsin Effect in Intact Goldfish Cones

Previously, we found salamander cones to be quite sensitive to constitutive phototransduction activity in darkness, such that even a low fractional content of apo-opsin will lead to equivalent background-light adaptation. This property allowed us to assay, albeit only roughly, the amount of apo-opsin in salamander cones [12]. However, this approach does not work for goldfish cones, as discussed below.

First, we outline some basic properties of goldfish L, M and S cones that we found (cf. striped bass [44] and carp [45]). These cone subtypes differed by a ~20-fold-range in dim-flash sensitivity at their respective λ_{max} (Figure 5A), with a corresponding half-saturating flash intensity (σ) of 4,016 ± 901 (mean ± SD, n=13), 676 ± 481 (n=8) and 231 ± 99 (n=8) photons μm^{-2} with 620-nm, 540-nm, and 450-nm flashes, respectively (Figure 5A); thus, L cones were the least sensitive. Their corresponding saturated light responses were 16.7 ± 4.1 pA (n=10), 11.8 ± 6.2 pA (n=8) and 9.7 ± 2.8 pA (n=8), correlated with their outer-segment surface areas (R^2 = 0.99, Table S1). The tiny single-photon responses were unresolvable, but could be estimated from average dim-flash-response amplitudes, flash intensities and effective collecting areas (Figure 5B; Table S1), giving 2.1 ± 1.4 fA (n=13) for L cones, 10.9

± 13.6 fA (n=8) for M cones, and 21.3 ± 7.9 fA (n=8) for S cones. In comparison, goldfish rods had a dark current of 9.2 ± 2.8 pA (n=4), σ of 14 ± 4 photons μm^{-2} at λ_{max} (n=4), and a single-photon response of 1.00 ± 0.30 pA (n=4). Thus, goldfish cone subtypes (with the UV-subtype still unknown) were 50- to 500-fold less sensitive than goldfish rods.

Figure 5C shows incremental-flash-on-background experiments. In each cone subtype, flash sensitivity decreases with background light intensity according to the Weber-Fechner law, $S_F/S_F^D = I_o/(I_B + I_o)$, where S_F^D is flash sensitivity in darkness, S_F is flash sensitivity in background light of intensity I_B, and I_o is background intensity that reduces flash sensitivity by half. Collected results gave an I_o of 21,739 ± 8,002 (n = 8), 1,049 ± 348 (n = 6) and 791 ± 338 (n = 4) photons μm^{-2} s^{-1} for L, M, and S cones, respectively. Converting them into equivalent isomerizations gives ~42,000 ± 15,000 isomerizations s^{-1} in L cones, 1,400 ± 500 isomerizations s^{-1} in M cones, and 1,300 ± 600 isomerizations s^{-1} in S cones. As such, this is quite different from salamander cones, where, for example, the I_o value for L cones is only ~1,200 isomerizations s^{-1} [6,12]. This large difference in I_o appears to come mostly from a difference in single-photon-response properties between salamander and goldfish cones. The single-photon response of salamander L cones has an averaged time integral of 7.24 fC [6,27], more than 20 times that of goldfish L cones (0.31 fC). Hence, a given background light has a far stronger effect in salamander cones than in goldfish cones, resulting in a smaller Weber constant I_o in salamander cones. Such a disparity in I_o value exists for the same reason in some mammals, such as between primate and ground squirrel cones [46].

Given the I_o values in goldfish L, M, and S cones being >10-fold higher than the respective transduction noise (see previous section), dark apo-opsin activity is insignificant in producing background-light adaptation, explaining why we did not use this phenomenon for calculating apo-opsin content. Thus, apo-opsin in dark-adapted goldfish cones mostly just reduces the probability of photon capture. We tested this possibility by measuring dark-adapted sensitivity in intact goldfish L cones before and after applying exogenous chromophore (STAR★METHODS) to regenerate any apo-opsin (Figure 5, D-G). We found an increase in sensitivity with A_1- or A_2- chromophore, giving ~25 ± 12% apo-opsin in dark-adapted L cones – broadly consistent with our micropectrophotometric data. Likewise, we observed no obvious sensitivity decrease over time, starting at ~15 min after cell dissociation into Ringer solution, prior to adding exogenous chromophore. We did not perform these experiments in M and S cones, partly because of their scarcity and the difficulty of sustaining stable recordings while applying chromophore. Given the microspectrophotometric data, however, we do not expect any significant chromophore-induced change in their sensitivity.

DISCUSSION

In this work, we found much higher constitutive cone apo-opsin activity than spontaneous pigment isomerization in producing dark GTP-dependent transduction noise. This led us to revisit past work on cone noise. Previously, another group studied salamander cones with the truncated-cone preparation, but did not use it to extract dark-noise parameters [6]. Instead, based on power spectral analysis of recorded noise from intact salamander L cones, they estimated the total dark GTP-dependent transduction activity to

be equivalent to ~600 isomerizations s^{-1} $cell^{-1}$ [6], attributing it entirely to spontaneous holo-pigment isomerization. From our work here, however, this noise may mostly come from constitutive apo-opsin activity instead. To check further, we made the following calculations. Salamander L cone pigment, estimated at 2.7×10^8 molecules $cell^{-1}$ in total [12], comprises on average 48% A_1-component (λ_{max} at 562 nm) and 52% A_2-component (λ_{max} at 620 nm) [12]. Following the approach described in Results – predicting the molecular rate constants of spontaneous isomerization for holo-pigments based on λ_{max} [38] – we obtained, for salamander L cones at room temperature, ~4.4 spontaneous events sec^{-1} for A_1- and ~65.5 spontaneous events sec^{-1} for A_2-pigment, thus altogether ~70 events s^{-1}. For salamander L cone apo-opsin, constituting ~10% of total pigment [12], with each molecule giving 1.67×10^{-5} dark equivalent isomerizations sec^{-1} [14], or ~451 dark equivalent isomerizations sec^{-1} overall. Thus, altogether, the total dark transduction activity is ~(70 + 451) = 521 dark equivalent isomerizations sec^{-1}, fairly similar to the ~600 events sec^{-1} derived from power spectral analysis [6]. It is also possible to calculate the noise variance associated with this dark transduction activity, which also matches the reported noise fairly well [6] (STAR★METHODS), supporting the notion that apo-opsin instead of spontaneous isomerization may be the predominant noise source.

The above exercise highlights the potential ambiguity in power spectral analysis. It might be argued that the unitary amplitude and waveform of the flash response should be quite different from those of opsin-triggered events. However, this may not necessarily be the case. It is now clear that, in rods, each active rhodopsin activates only 10–20 rod transducin/PDE effector complexes [16,47]. In cones, the amplification factor in this step is still unknown, but considering the overall photosensitivity being generally ~10^2 times lower in cones than in rods [48] – indeed, 500 times lower specifically in goldfish L cones (see Results) – it is not unthinkable that an active cone-pigment molecule activates *on average* only around one, or lower, cone transducin/PDE effector complex. If so, the single-photon response in L cones can only be described probabilistically, much like the situation in olfactory transduction [49]. Furthermore, it is almost certain that cone apo-opsin's constitutive activity has very low gain, as found for rod apo-opsin which, when active, leads at most to a single rod transducin/PDE effector complex [16]. Thus, constitutively active holo-pigment and apo-opsin may produce unitary signals with similar or broadly similar amplitudes and kinetics, rendering them potentially difficult to be distinguished from each other with power spectral analysis or synaptic filtering. The similar signals from photoexcited holo-pigment and from constitutive apo-opsin may also elevate the cone visual threshold.

The substantial percentage (~30%) of apo-opsin in dark-adapted L-cones is surprising and may call for a significant correction of previous microspectrophotometric measurements. Such studies have traditionally overlooked apo-opsin's presence, consequently underestimating the overall pigment content. This correction is less important for M cones and probably negligible for S cones. Obviously, it remains to be validated that our findings in goldfish apply generally to other species, including mammals, and to A_1- and A_2-chromophores.

Given L-cone pigment's significant tendency to dissociate spontaneously, it is surprising in our microspectrophotometric experiments that the apo-opsin content of L cones did not increase progressively with time after isolation from the retina and pigment epithelium into chromophore-free saline (previously, we have found the same in salamander L cones based on sensitivity measurements; see p. 882 in [12]). In principle, holo-pigment and apo-opsin in cones should be in some dynamic equilibrium in darkness, with their ratio being dependent on the free-chromophore pool accessible to the pigment. Our earlier finding in salamander L cones has been that exogenously-applied excess 9-*cis*-retinal is able to replace the endogenous chromophore with a time constant of ~160 min [12], suggesting that endogenous chromophore dissociates from the holo-pigment at least as fast. To explain these seemingly contradictory findings, we speculate that the endogenous chromophore, being hydrophobic, actually stays in close proximity once dissociated from a pigment molecule and tends to rebind the apo-opsin afterwards. With excess exogenous chromophore around, however, such as in a chromophore-exchange experiment, the exogenous chromophore would readily out-compete the dissociated endogenous chromophore to lead to exchange. In any case, it appears at least observationally that the L-cone apo-opsin content does not increase after cell isolation, unless this happened and was complete in ~15 min, the earliest time of sensitivity measurement (see Results).

Finally, we have quantified the constitutive molecular activity of goldfish L and M cone apo-opsins. For L-cone apo-opsin, it is 1.08×10^{-5} equivalent isomerizations s^{-1}, quite close to the 1.67×10^{-5} equivalent isomerizations s^{-1} for photobleached opsin in salamander L cones estimated by others using a different approach, both at room temperature [14]. For goldfish M cone apo-opsin, we found a molecular constitutive activity of 4.86×10^{-6} equivalent isomerizations s^{-1}, with no corresponding measurement in another animal species available for comparison. The ~2-fold difference in molecular activity between L- and M-cone apo-opsins probably should not be taken too literally at present; it may just reflect measurement uncertainty. As for S apo-opsin, this parameter remains unknown.

STAR★METHODS

RESOURCE AVAILABILITY

Lead Contact—Further information and requests for resources and reagents should be directed to and will be fulfilled by the Lead Contact, King-Wai Yau (kwyau@jhmi.edu).

Materials Availability—This study did not generate new unique reagents.

Data and Code Availability—Original data is available from the corresponding author on request.

EXPERIMENTAL MODEL AND SUBJECT DETAILS

All animal experiments were conducted according to protocols approved by the Institutional Animal Care and Use Committee at Johns Hopkins University. Goldfish (adult pond comets measuring) were obtained from Ozark Fisheries (Stoutland, MO) and housed in an aquarium under a 12:12 light:dark cycle. Determining the age of each goldfish is challenging because

they are raised in a pond with fish of a range of ages. We used mature goldfish that were identified based on their metallic orange color and length characteristic of adult fish (>5 inches long, >18 months old). Determining the gender of each goldfish is also subtle. In general, male goldfish had a long and slender pectoral fin, while females had pectoral fins that were short and more rounded.

METHOD DETAILS

Suction-pipette recordings—The night before an experiment, an individual goldfish was kept in total darkness in a separate aquarium in the recording room. Goldfish eyecups were stored in fish Ringer's: (mM) 130 NaCl, 2.6 KCl, 1 $MgCl_2$, 1 $CaCl_2$, 10 HEPES (pH 7.8), 0.02 EDTA, and 10 D-glucose on ice until use over many hours. When needed, a small piece was cut from the eyecup, and the retina removed, chopped, and transferred to the recording chamber perfused with fish Ringer's. Suction-pipette recordings were performed as previously described [38,40,50]. Briefly, guided by an infrared-sensitive camera, the outer segment of an isolated single cone was drawn into a tight-fitting glass pipette coated with tri-*n*-butylchlorosilane (Pfaltz and Bauer Inc., Waterbury, CT) and filled with fish Ringer's. Membrane current was measured with a current-to-voltage amplifier (Axopatch 200B; Axon Instruments). Signals were low-pass filtered at 1 kHz and 20 Hz (RC filter; Krohnhite 3340) and sampled at 2 kHz. For synchronization with light stimuli, the 1-kHz channel was compared with the 20-Hz channel in order to correct the time delay caused by filtering. All experiments were performed at ~23°C.

Truncated-cone recordings—A glass probe was brought close to a cone held by its outer segment and part of the inner segment in a suction-pipette electrode. A lateral stroke of the glass probe sheared off most of the inner segment and the cell body of the recorded cone. As a result, an open-ended outer segment/inner segment was obtained. Occasionally, a second stroke was needed when the first trial failed. The open end of the outer segment/inner segment was brought close to the outlet of a perfusion tubing array connected to multiple solution reservoirs. Solenoid Valve (Lee Company) and ValveLink 8 (AutoMate Scientific, Inc.) controlled solution switching and perfusion was driven by gravity.

The recording electrode was filled with (in mM): 130 NaCl, 0.05 $CaCl_2$, 1 $MgCl_2$, 10 HEPES (pH 7.8), 1 EGTA, and 10 D-glucose, with the calculated free [Ca^{2+}] being 0.75 nM. The low Ca^{2+} concentration in the pipette was intended for minimizing any Ca^{2+} influx through the CNG channels into the outer segment. The composition of the pseudo-intracellular (bath) solution is: (in mM) 135 L-Arginine, 135 L-Glutamic Acid, 1 $MgCl_2$, 0.66 $CaCl_2$, 10 HEPES (pH 7.8), 1 BAPTA, with the calculated buffered free [Ca^{2+}] concentration of 390 nM, so chosen as to match the free Ca^{2+} concentration measured optically in the intact salamander cone OS in darkness [51]. L-Arginine and L-Glutamic Acid replaced NaCl and KCl to prevent activation of the sodium-calcium-potassium exchanger current, which could complicate analyses of the cGMP-dissipation rate. GTP-Mg^{2+}, ATP-Mg^{2+} and cGMP-Na^{+} were dissolved in water and freshly prepared. IBMX was dissolved in DMSO. The final concentrations of ATP, GTP and IBMX were obtained after dilution with the pseudo-intracellular solution. The membrane potential was held at 0 mV.

Our truncated-cone experiments consisted predominantly of monitoring PDE activity by measuring membrane current to indicate kinetic changes in cGMP concentrations, starting with very high cGMP concentrations. As such, there were no steady-state current recordings at low cGMP concentrations in darkness to be amenable to power spectral analysis for comparison with previous work on cone noise. Additionally, in chromophore-treatment experiments with intact L cones, we needed to focus on measuring dim-flash responses within a narrow time window (5–10 min) before and after adding chromophore. Longer recordings were complicated by changes in the dark current due to structural damage or slight movement of the cell within the pipette, which precluded any meaningful analysis of dark noise power spectra.

Cell identification and light stimuli—In goldfish, there are single cones and double cones. Single cones consist of L, M, S, and UV cones. Double cones are a pair of L and M cones. Identifications of cone subtypes were based on their spectral sensitivity: L, M, S, and UV cones were most sensitive to wavelengths of 623, 537, 447, and 360 nm, respectively [18,26]. Cones were stimulated with calibrated 10-ms flashes near their optimal monochromatic wavelengths. Dim-flash responses were averaged from 40–60 repeated trials and bright-flash responses were averaged from 10–20 repeated trials.

Estimating cellular thermal isomerization rates in dark-adapted goldfish L, M, and S cones—The following calculations are based on the pigment-noise theory described in [38]:

1) L cones: λ_{max} = 623 nm: $E_a = 0.84 \times hc/\lambda_{max} = 6.41 \times 10^{-23}$ kcal molecule^{-1} = 38.6 kcal mol^{-1}

T = 296.15 °K

$\exp[-E_a/(RT)] = 3.41 \times 10^{-29}$

$$f_{\geq Ea} = e^{\frac{-0.84hc}{RT\lambda_{\max}}} \sum_{1}^{m} \frac{1}{(m-1)!}\left(\frac{0.84hc}{RT\lambda_{\max}}\right)^{m-1} = 3.07 \times 10^{-3}$$

Pre-exponential factor (A) = 1.88×10^{-4}

Thus, molecular thermal isomerization rate constant = $A \times f_{\geq Ea} = 5.78 \times 10^{-7}$ sec^{-1} molecule^{-1}

Cellular pigment content = Outer-Segment Volume × Pigment Concentration (assuming 32% apo-opsin content) = (2.02×10^{-13} L) × (3.5 mM×0.68) × $N_{Avogadro} = 2.90 \times 10^8$ pigment molecules

Therefore, cellular rate of thermal isomerization = Molecular rate constant × pigment content = (5.78×10^{-7} isomerizations sec^{-1} molecule^{-1}) × (2.90×10^8 pigment molecules cell^{-1}) = **167 thermal isomerizations sec^{-1} cell^{-1}**

2) M-cones: λ_{max} = 537 nm: $E_a = 0.84 \times hc/\lambda_{max} = 7.43 \times 10^{-23}$ kcal molecule^{-1} = 44.8 kcal mol^{-1}

T = 296.15 °K

$\exp[-E_a/(RT)] = 9.42 \times 10^{-34}$

$$f \geq Ea = e^{\frac{-0.84hc}{RT\lambda_{\max}}} \sum_1^m \frac{1}{(m-1)!}\left(\frac{0.84hc}{RT\lambda_{\max}}\right)^{m-1} = 4.74 \times 10^{-5}$$

Pre-exponential factor (A) = 1.88×10^{-4}

Thus, molecular thermal isomerization rate constant = $A \times f_{\geq Ea} = 8.91 \times 10^{-9}$ sec^{-1} molecule^{-1}

Cellular pigment content = Outer-Segment Volume × Pigment Concentration (assuming 3% apo-opsin content) = (1.43×10^{-13} L) × (3.5 mM×0.97) × $N_{Avogadro} = 2.92 \times 10^8$ pigment molecules

Therefore, cellular rate of thermal isomerization = Molecular rate constant × pigment content = (8.91×10^{-9} isomerizations sec^{-1} molecule^{-1}) × (2.92×10^8 pigment molecules cell^{-1}) = **3 thermal isomerizations sec^{-1} cell^{-1}**

3) S cones: λ_{max} = 447 nm: $E_a = 8.93 \times 10^{-23}$ kcal molecule^{-1} = 53.8 kcal mol^{-1}

T = 296.15 °K

$\exp[-E_a/(RT)] = 2.11 \times 10^{-40}$

$$f \geq Ea = e^{\frac{-0.84hc}{RT\lambda_{\max}}} \sum_1^m \frac{1}{(m-1)!}\left(\frac{0.84hc}{RT\lambda_{\max}}\right)^{m-1} = 2.82 \times 10^{-8}$$

Pre-exponential factor (A) = 1.88×10^{-4}

Thus, molecular thermal isomerization rate constant = $A \times f_{\geq Ea} = 5.30 \times 10^{-12}$ sec^{-1} molecule^{-1}

Cellular pigment content = Outer-Segment Volume × Pigment Concentration (unknown apo-opsin content) = (1.72×10^{-13} L) × (3.5 mM) × $N_{Avogadro} = 3.63 \times 10^8$ pigment molecules

Therefore, cellular rate of thermal isomerization = Molecular rate constant × pigment content = (5.30×10^{-12} isomerizations sec^{-1} molecule^{-1}) × (3.63×10^8 pigment molecules cell^{-1}) = **0.002 thermal isomerizations sec^{-1} cell^{-1}**

Microspectrophotometry (MSP)—Optical density was measured on a previously described instrument [52–54]. At the beginning of an experiment, a dark-adapted goldfish retina was peeled from the retinal pigment epithelium, chopped and triturated in the recording solution under infrared illumination. The solution containing retinal fragments

as well as isolated intact cells was placed on a quartz coverslip window coated with concanavalin A (Sigma-Aldrich) located at the bottom of a 2 mm-deep Plexiglass recording chamber. Cells were allowed to settle and adhere to the quartz window for about 5 min. Afterwards, the chamber was perfused at 4 mL/min with recording solution. A baseline absorbance spectrum was measured from an area adjacent to the selected cell. The outer segment was then brought into the beam path with the long axis of the slit oriented parallel to the long axis of the outer segment, and an absorbance measurement in this area was made, comprising four spectral scans. From these measurements, the dark-adapted optical density was calculated according to Beer's law. Afterwards, perfusion was paused and 11-*cis*-retinal (10-μM final concentration) was injected into the recording chamber and incubated with the cell for 15 min before the optical density was measured again from the same cell. The time lapse starting at the isolation of the retina from the retinal pigment epithelium to the measurement of the absorption spectrum (prior to 11-cis-retinal addition) was noted. Because of their orientation in the outer segments, visual pigments absorb maximally when the polarization of the measurement beam was transverse (T, as opposed to longitudinal, L) to the length of the outer segment. Thus, to increase the signal, the data from the L and M cones were recorded in T-polarization. In the S cones where there is a significant overlap between the pigment spectrum and that of free exogenous chromophore, we recorded in both T and L polarization and analyzed the difference spectra (T minus L) between the two polarizations. This method had the advantage that we could eliminate the absorbance from free exogenous chromophore that absorbs equally in T and L polarization, but came with the cost of an overall reduction in the signal.

Calculation of apo-opsin content in dark-adapted goldfish cones from MSP measurements—Fractional apo-opsin content was calculated by first determining the amount of apo-opsin regenerated into pigment by quantifying a cone's difference spectrum from microspectrophotometry [(post-chromophore-treatment spectrum) minus (pre-treatment spectrum); see Results]. A measurable difference spectrum (positive values) that could be fit with an A_1 template [55] indicated an increase in photon capture from newly-formed pigment. Part of the observed increase in photon capture was due to a higher extinction coefficient of 11-*cis*-retinal (A_1) pigment relative to that of the goldfish's native 11-cis-dehydroretinal (A_2) pigment [12,18,42]. As such, the difference spectrum (representing A_1 pigment) needs to be adjusted by multiplication with the A_2/A_1-extinction-coefficient ratio [12]. It is generally thought that A_2 pigments have a molar extinction coefficient of ~30,000 L mol^{-1} cm^{-1} based primarily on *in vitro* measurements with A_2-based rhodopsin [42] and that the molar extinction coefficient of A_1-based pigments is ~42,000 L mol^{-1} cm^{-1} [56,57]. Thus, for adjustment, we multiplied the difference spectrum's peak optical density by the A_2/A_1-extinction-coefficient ratio (30,000/42,000 = 0.71). The fractional apo-opsin content was then calculated as the A_1-pigment's adjusted peak optical density divided by the total peak optical density (i.e., A_1 pigment plus endogenous A_2 pigment). Finally, to calculate the absolute number of apo-opsin molecules, we multiplied the fractional apo-opsin content with the outer-segment volume of a goldfish L or M cone (Table S1) and the packing density of visual pigment (nominally ~3.5 mM, [18,43]).

As a side note, it has been speculated [18] based on microspectrophotometry that the goldfish L-cone pigment might have a slightly higher extinction coefficient (~40,000 $Lmol^{-1}cm^{-1}$) compared to M- and S-cone pigments (~30,000 $Lmol^{-1}cm^{-1}$) despite all using A_2 chromophore. This possibility was based on a theoretical approximation [58] and has not been substantiated by standard methods [56]. If ~40,000 $Lmol^{-1}cm^{-1}$ had been used in our calculation of apo-opsin content in goldfish L cones, the resulting estimate of average apo-opsin content in goldfish L cones would be even higher (~42% instead of ~32%).

Application of chromophore during suction-pipette recordings from isolated, dark-adapted goldfish L cones, and calculation of apo-opsin content in them—Chromophore (either A_1 or A_2) was applied to goldfish cones during a suction-pipette recording experiment with the outer segment drawn into the pipette. To avoid adsorption of the hydrophobic chromophore to plastic, we used stainless steel hypodermic tubing and a custom-fabricated stainless-steel recording chamber. The chromophore (10-μM 11-*cis*-retinal A_1 or 11-cis-dehydroretinal A_2 in Fish Ringer's containing 0.1% lipid-free BSA) was held in a glass syringe reservoir in darkness on the microscope stage until needed. To apply chromophore, a 3-way valve was switched on to allow chromophore to flow into the chamber until the chromophore solution had completely replaced the initial bath solution (thus reaching 10-μM final concentration). Dim-flash responses were measured before chromophore exposure and immediately after a 10-min exposure period.

The fractional apo-opsin content in the recorded L cones can be calculated in a similar manner as for the microspectrophotometric experiments. Because apo-opsin's constitutive activity does not appear to trigger adaptation in goldfish cones (see Results), we can estimate a cone's increase in photon capture directly from the chromophore-treatment-induced increase in photosensitivity. We first determined the increase in 620-nm photon capture from the change in absolute sensitivity (mean dim-flash response amplitude / flash strength) quantified as [(post-chromophore-treatment sensitivity) minus (pre-treatment sensitivity), see also Results]. A measurable increase in sensitivity indicated an increase in photon capture from newly-formed pigment after regenerating the apo-opsin population present in darkness. Unlike the full-spectrum measurements taken in microspectrophotometry experiments, only 620-nm light was used to assess the change in physiological sensitivity. In experiments with A_1-chromophore treatment, we needed to adjust the observed change in 620-nm sensitivity to account for the blue-shifted λ_{max} of L-cone A_1 pigment (562 nm, [12]) by multiplication with the 620-nm A_2/A_1-sensitivity ratio (1.67) and to account for the difference in extinction coefficient between A_1 and A_2 pigment by multiplication with the A_2/A_1-extinction-coefficient ratio (0.71). Finally, fractional apo-opsin content was calculated from the sensitivity increase (after 620-nm sensitivity ratio and extinction-coefficient-ratio-adjustment) divided by total post-chromophore-treatment sensitivity (i.e., resulting from the sum of peak sensitivities from A_1 and A_2 pigments). In experiments with A_2-chromophore, the fractional apo-opsin content was directly evaluated from the increase in sensitivity at 620 nm [i.e., (change in sensitivity from chromophore treatment) / (final post-chromophore-treatment sensitivity)] because the newly-formed pigment had a λ_{max} and an extinction coefficient identical to those of the goldfish's endogenous A_2 pigment.

Estimation of noise variance associated with dark transduction activity in salamander L cones—The dark noise variance in salamander L cones was 0.18 pA^2 [6]. To test the possibility that this noise consisted of apo-opsin signaling in addition to spontaneous holo-pigment isomerization, we estimated the noise variance in a salamander L cone as follows. According to Campbell's theorem, the steady-noise variance is equal to $v \times \int [f(t)]^2 dt$ and the steady-noise mean is equal to $v \times \int f(t) dt$, where *f(t)* is the single-photon response waveform and v is the average frequency of randomly-occurring events [59]. By expressing *f(t)* as $a \times \hat{f}(t)$, where $\hat{f}(t)$ is normalized *f(t)* at transient peak and *a* is the single-photon response amplitude [16], we obtain:

$$\text{Steady noise variance} = \text{Steady noise mean} \times a / \left\{ \int f(t) dt / \int [f(t)]^2 dt \right\}$$

The denominator is called the "shape factor" and its value is mostly between 1 and 2 for simple waveforms [59]. For simplicity, we use the value of unity (which would be the case for a square wave). Thus, Steady noise variance = Steady noise mean × $a = v \int f(t) dt \times a$. As described in Discussion, then, for salamander L cones, with $\int f(t) dt$ = 0.00724 pA·sec and v = 521 dark "equivalent" isomerizations sec^{-1} (~4.4 A_1-pigment isomerizations sec^{-1} + 65.5 A_2-pigment isomerizations sec^{-1} + 451 "equivalent" isomerizations sec^{-1} from apo-opsin activity), and *a* = 0.04 pA (based on the approximate scenario in Discussion of an equal unitary-response amplitude for the apo-opsin-triggered event and the single-photon response). Thus, our estimated dark noise variance for salamander red cones is 521 events sec^{-1} × 0.00724 pA·sec × 0.04 pA ~0.15 pA^2, which is fairly close to the measured value of 0.18 pA^2 [6].

QUANTIFICATION AND STATISTICAL ANALYSIS

All values presented are mean±S.D. For physiological recordings, data with obvious changes in cell state during recording (e.g., abrupt shift in dark current or kinetics from mechanical damage caused by the pipette) were excluded from analyses.

Supplementary Material

Refer to Web version on PubMed Central for supplementary material.

ACKNOWLEDGMENTS

We thank Wendy Yue, Zuying Chai, Michael Tri Do, and Rongchang Li for comments. This work was supported by grant R01 EY06837 (U.S. National Eye Institute) (K.-W.Y.) and R01 EY01157 (M.C.C.), the Antȯnio Champalimaud Vision Award (Champalimaud Foundation, Portugal) and the Beckman-Argyros Award in Vision Research (Arnold and Mabel Beckman Foundation), both to K.-W.Y., as well as the Visual Science Training Program Fellowship, EY007143 (National Eye Institute) to D.S.

REFERENCES

1. Baylor DA, Matthews G, and Yau KW (1980). Two components of electrical dark noise in toad retinal rod outer segments. J. Physiol 309, 591–621. Available at: http://doi.wiley.com/10.1113/jphysiol.1980.sp013529. [PubMed: 6788941]
2. Baylor DA, Nunn BJ, and Schnapf JL (1984). The photocurrent, noise and spectral sensitivity of rods of the monkey Macaca fascicularis. J. Physiol 357, 575–607. Available at: http://www.ncbi.nlm.nih.gov/pubmed/6512705 [Accessed October 20, 2018]. [PubMed: 6512705]

3. Jones GJ (1998). Membrane current noise in dark-adapted and light-adapted isolated retinal rods of the larval tiger salamander. J. Physiol 511, 903–913. Available at: http://www.ncbi.nlm.nih.gov/pubmed/9714869 [Accessed March 21, 2020]. [PubMed: 9714869]
4. Rieke F, and Baylor DA (1996). Molecular origin of continuous dark noise in rod photoreceptors. Biophys. J 71, 2553–2572. [PubMed: 8913594]
5. Lamb TD, and Simon EJ (1977). Analysis of electrical noise in turtle cones. J. Physiol 272, 435–468. Available at: http://www.ncbi.nlm.nih.gov/pubmed/592199 [Accessed September 5, 2019]. [PubMed: 592199]
6. Rieke F, and Baylor DA (2000). Origin and functional impact of dark noise in retinal cones. Neuron 26, 181–186. [PubMed: 10798402]
7. Sampath AP, and Baylor DA (2002). Molecular mechanism of spontaneous pigment activation in retinal cones. Biophys. J 83, 184–193. Available at: http://www.pubmedcentral.nih.gov/articlerender.fcgi?artid=1302138%7B&%7Dtool=pmcentrez%7B&%7Drendertype=abstract. [PubMed: 12080111]
8. Holcman D, and Korenbrot JI (2005). The limit of photoreceptor sensitivity: molecular mechanisms of dark noise in retinal cones. J. Gen. Physiol 125, 641–660. [PubMed: 15928405]
9. Angueyra JM, and Rieke F. (2013). Origin and effect of phototransduction noise in primate cone photoreceptors. Nat. Neurosci 16, 1692–1700. Available at: http://www.nature.com/articles/nn.3534 [Accessed April 19, 2019]. [PubMed: 24097042]
10. Schnapf JL, Nunn BJ, Meister M, and Baylor DA (1990). Visual transduction in cones of the monkey Macaca fascicularis. J. Physiol 427, 681–713. Available at: http://www.ncbi.nlm.nih.gov/pubmed/2100987 [Accessed August 21, 2019]. [PubMed: 2100987]
11. Schneeweis DM, and Schnapf JL (1999). The photovoltage of macaque cone photoreceptors: adaptation, noise, and kinetics. J. Neurosci 19, 1203–1216. [PubMed: 9952398]
12. Kefalov VJ, Estevez ME, Kono M, Goletz PW, Crouch RK, Cornwall MC, and Yau K-W (2005). Breaking the covalent bond — a pigment property that contributes to desensitization in cones. Neuron 46, 879–890. Available at: http://linkinghub.elsevier.com/retrieve/pii/S0896627305004046. [PubMed: 15953417]
13. Matsumoto H, Tokunaga F, and Yoshizawa T. (1975). Accessibility of the iodopsin chromophore. Biochim. Biophys. Acta - Gen. Subj 404, 300–308. Available at: https://www.sciencedirect.com/science/article/pii/0304416575903372 [Accessed September 27, 2019].
14. Cornwall MC, Matthews HR, Crouch RK, and Fain GL (1995). Bleached pigment activates transduction in salamander cones. J. Gen. Physiol 106, 543–57. Available at: http://www.ncbi.nlm.nih.gov/pubmed/8786347 [Accessed April 19, 2019]. [PubMed: 8786347]
15. Surya A, Foster KW, and Knox BE (1995). Transducin activation by the bovine opsin apoprotein. J. Biol. Chem 270, 5024–5031. [PubMed: 7890610]
16. Yue WWS, Silverman D, Ren X, Frederiksen R, Sakai K, Yamashita T, Shichida Y, Cornwall MC, Chen J, and Yau K-W (2019). Elementary response triggered by transducin in retinal rods. Proc. Natl. Acad. Sci 116, 5144–5153. Available at: http://www.ncbi.nlm.nih.gov/pubmed/30796193 [Accessed September 27, 2019]. [PubMed: 30796193]
17. Cornwall MC, and Fain GL (1994). Bleached pigment activates transduction in isolated rods of the salamander retina. J. Physiol 480, 261–279. [PubMed: 7532713]
18. Hárosi FI, and MacNichol EF (1974). Visual pigments of goldfish cones. Spectral properties and dichroism. J. Gen. Physiol 63, 279–304. Available at: http://www.ncbi.nlm.nih.gov/pubmed/4817352 [Accessed October 20, 2018]. [PubMed: 4817352]
19. Jones GJ, Fein A, Macnichol EF, and Carter Cornwall M. (1993). Visual pigment bleaching in isolated salamander retinal cones: Microspectrophotometry and light adaptation. J. Gen. Physiol 102, 483–502. Available at: http://www.ncbi.nlm.nih.gov/pubmed/8245820 [Accessed April 13, 2020]. [PubMed: 8245820]
20. Koutalos Y, Nakatani K, Tamura T, and Yau KW (1995). Characterization of guanylate cyclase activity in single retinal rod outer segments. J. Gen. Physiol 106, 863–890. Available at: http://www.ncbi.nlm.nih.gov/pubmed/8648296 [Accessed April 13, 2020]. [PubMed: 8648296]

21. Koutalos Y, Nakatani K, and Yau KW (1995). Cyclic GMP diffusion coefficient in rod photoreceptor outer segments. Biophys. J 68, 373–382. Available at: http://www.ncbi.nlm.nih.gov/pubmed/7536055 [Accessed October 20, 2018]. [PubMed: 7536055]
22. Koutalos Y, Nakatani K, and Yau KW (1995). The cGMP-phosphodiesterase and its contribution to sensitivity regulation in retinal rods. J. Gen. Physiol 106, 891–921. Available at: http://www.ncbi.nlm.nih.gov/pubmed/8648297 [Accessed April 13, 2020]. [PubMed: 8648297]
23. Yau KW, and Nakatani K. (1985). Light-suppressible, cyclic GMP-sensitive conductance in the plasma membrane of a truncated rod outer segment. Nature 317, 252–255. Available at: http://www.ncbi.nlm.nih.gov/pubmed/2995816 [Accessed March 21, 2020]. [PubMed: 2995816]
24. Nakatani K, and Yau K-W (1986). Light-suppressible cGMP-activated current recorded from a dialyzed cone preparation. Invest. Ophthalmol. Vis. Sci 27, 300.
25. Balkema GW, and Bunt-Milam AH (1982). Cone outer segment shedding in the goldfish retina characterized with the 3H-fucose technique. Invest. Ophthalmol. Vis. Sci 23, 319–31. Available at: http://www.ncbi.nlm.nih.gov/pubmed/7107159 [Accessed April 19, 2019]. [PubMed: 7107159]
26. Palacios AG, Varela FJ, Srivastava R, and Goldsmith TH (1998). Spectral sensitivity of cones in the goldfish, Carassius auratus. Vision Res. 38, 2135–46. Available at: http://www.ncbi.nlm.nih.gov/pubmed/9797974 [Accessed October 20, 2018]. [PubMed: 9797974]
27. Perry RJ, and McNaughton PA (1991). Response properties of cones from the retina of the tiger salamander. J. Physiol 433, 561–87. Available at: http://www.ncbi.nlm.nih.gov/pubmed/1841958 [Accessed October 20, 2018]. [PubMed: 1841958]
28. Haynes L, and Yau KW (1985). Cyclic GMP-sensitive conductance in outer segment membrane of catfish cones. Nature 317, 61–4. Available at: http://www.ncbi.nlm.nih.gov/pubmed/2993914 [Accessed October 21, 2018]. [PubMed: 2993914]
29. Haynes LW, and Yau KW (1990). Single-channel measurement from the cyclic GMP-activated conductance of catfish retinal cones. J. Physiol 429, 451–481. Available at: https://pubmed.ncbi.nlm.nih.gov/1703573/ [Accessed August 6, 2020]. [PubMed: 1703573]
30. Lerea CL, Bunt-Milam AH, and Hurley JB (1989). Alpha transducin is present in blue-, green-, and red-sensitive cone photoreceptors in the human retina. Neuron 3, 367–76. Available at: http://www.ncbi.nlm.nih.gov/pubmed/2534964 [Accessed October 20, 2018]. [PubMed: 2534964]
31. Fan J, Woodruff ML, Cilluffo MC, Crouch RK, and Fain GL (2005). Opsin activation of transduction in the rods of dark-reared Rpe65 knockout mice. J. Physiol 568, 83–95. [PubMed: 15994181]
32. Fan J, Sakurai K, Chen CK, Rohrer B, Wu BX, Yau KW, Kefalov V, and Crouch RK (2010). Deletion of GRK1 causes retina degeneration through a transducin-independent mechanism. J. Neurosci 30, 2496–2503. [PubMed: 20164334]
33. Elias RV, Sezate SS, Cao W, and McGinnis JF (2004). Temporal kinetics of the light/dark translocation and compartmentation of arrestin and alpha-transducin in mouse photoreceptor cells. Mol. Vis 10, 672–81. Available at: http://www.ncbi.nlm.nih.gov/pubmed/15467522 [Accessed August 6, 2020]. [PubMed: 15467522]
34. Kennedy MJ, Dunn FA, and Hurley JB (2004). Visual pigment phosphorylation but not transducin translocation can contribute to light adaptation in zebrafish cones. Neuron 41, 915–928. Available at: https://pubmed.ncbi.nlm.nih.gov/15046724/ [Accessed August 6, 2020]. [PubMed: 15046724]
35. Lobanova ES, Herrmann R, Finkelstein S, Reidel B, Skiba NP, Deng WT, Jo R, Weiss ER, Hauswirth WW, and Arshavsky VY (2010). Mechanistic basis for the failure of cone transducin to translocate: Why cones are never blinded by light. J. Neurosci 30, 6815–6824. Available at: https://pubmed.ncbi.nlm.nih.gov/20484624/ [Accessed August 6, 2020]. [PubMed: 20484624]
36. Zhang H, Cuenca N, Ivanova T, Church-Kopish J, Frederick JM, MacLeish PR, and Baehr W. (2003). Identification and light-dependent translocation of a cone-specific antigen, cone arrestin, recognized by monoclonal antibody 7G6. Investig. Ophthalmol. Vis. Sci 44, 2858–2867. Available at: https://pubmed.ncbi.nlm.nih.gov/12824223/ [Accessed August 6, 2020]. [PubMed: 12824223]
37. Haire SE, Pang J, Boye SL, Sokal I, Craft CM, Palczewski K, Hauswirth WW, and Semple-Rowland SL (2006). Light-driven cone arrestin translocation in cones of postnatal guanylate cyclase-1 knockout mouse retina treated with AAV-GC1. Investig. Ophthalmol. Vis. Sci 47,

3745–3753. Available at: https://pubmed.ncbi.nlm.nih.gov/16936082/ [Accessed August 6, 2020]. [PubMed: 16936082]

38. Luo D-G, Yue WWS, Ala-Laurila P, and Yau K-W (2011). Activation of visual pigments by light and heat. Science 332, 1307–12. Available at: http://www.ncbi.nlm.nih.gov/pubmed/21659602 [Accessed May 7, 2018]. [PubMed: 21659602]
39. Yue WWS, Frederiksen R, Ren X, Luo DG, Yamashita T, Shichida Y, Carter Cornwall M, and Yau KW (2017). Spontaneous activation of visual pigments in relation to openness/closedness of chromophore-binding pocket. Elife 6.
40. Silverman D, Chai Z, Yue WWS, Ramisetty SK, Bekshe Lokappa S, Sakai K, Frederiksen R, Bina P, Tsang SH, Yamashita T, et al. (2020). Dark noise and retinal degeneration from D190N-rhodopsin. Proc. Natl. Acad. Sci, 202010417. Available at: http://www.pnas.org/lookup/doi/10.1073/pnas.2010417117 [Accessed September 12, 2020].
41. Ala-Laurila P, Donner K, Crouch RK, and Cornwall MC (2007). Chromophore switch from 11-cis-dehydroretinal (A2) to 11-cis-retinal (A1) decreases dark noise in salamander red rods. J. Physiol 585, 57–74. Available at: http://www.pubmedcentral.nih.gov/articlerender.fcgi?artid=2375465%7B&%7Dtool=pmcentrez%7B&%7Drendertype=abstract. [PubMed: 17884920]
42. Brown PK, Gibbons IR, and Wald G. (1963). The visual cells and visual pigment of the mudpuppy, Necturus. J. Cell Biol 19, 79–106. Available at: http://www.jcb.org/cgi/doi/10.1083/jcb.19.1.79 [Accessed October 5, 2019]. [PubMed: 14069804]
43. Hárosi FI (1975). Absorption spectra and linear dichroism of some amphibian photoreceptors. J. Gen. Physiol 66, 357–382. [PubMed: 808586]
44. Miller JL, and Korenbrot JI (1993). Phototransduction and adaptation in rods, single cones, and twin cones of the striped bass retina: A comparative study. Vis. Neurosci 10, 653–667. [PubMed: 8338802]
45. Tachibanaki S, Tsushima S, and Kawamura S. (2001). Low amplification and fast visual pigment phosphorylation as mechanisms characterizing cone photoresponses. Proc. Natl. Acad. Sci. U. S. A 98, 14044–14049. [PubMed: 11707584]
46. Cao L-H, Luo D-G, and Yau K-W (2014). Light responses of primate and other mammalian cones. Proc. Natl. Acad. Sci. U. S. A 111, 2752–7. Available at: http://www.pnas.org/cgi/doi/10.1073/pnas.1400268111 [Accessed October 20, 2018]. [PubMed: 24550304]
47. Arshavsky VY, and Burns ME (2014). Current understanding of signal amplification in phototransduction. Cell. Logist 4, e29390. Available at: http://www.pubmedcentral.nih.gov/articlerender.fcgi?artid=4160332%7B&%7Dtool=pmcentrez%7B&%7Drendertype=abstract.
48. Luo D-G, Kefalov V, and Yau K-W (2008). 1.10 - Phototransduction in rods and cones. In The Senses: A Comprehensive Reference, Masland RH, Albright TD, Albright TD, Masland RH, Dallos P, Oertel D, Firestein S, Beauchamp GK, Bushnell MC, Basbaum AI, et al., eds. (New York: Academic Press), pp. 269–301. Available at: http://www.sciencedirect.com/science/article/pii/B9780123708809002589.
49. Bhandawat V, Reisert J, and Yau K-W (2005). Elementary response of olfactory receptor neurons to odorants. Science 308, 1931–1934. [PubMed: 15976304]
50. Baylor DA, Lamb TD, and Yau K-W (1979). Responses of retinal rods to single photons. J. Physiol 288, 613–634. [PubMed: 112243]
51. Sampath AP, Matthews HR, Cornwall MC, Bandarchi J, and Fain GL (1999). Light-dependent changes in outer segment free-Ca2+ concentration in salamander cone photoreceptors. J. Gen. Physiol 113, 267–77. Available at: http://www.ncbi.nlm.nih.gov/pubmed/9925824 [Accessed October 20, 2018]. [PubMed: 9925824]
52. Frederiksen R, Boyer NP, Nickle B, Chakrabarti KS, Koutalos Y, Crouch RK, Oprian D, and Cornwall MC (2012). Low aqueous solubility of 11-cis-retinal limits the rate of pigment formation and dark adaptation in salamander rods. J. Gen. Physiol 139, 493–505. Available at: http://www.ncbi.nlm.nih.gov/pubmed/22641642 [Accessed February 15, 2020]. [PubMed: 22641642]
53. Frederiksen R, Nymark S, Kolesnikov AV, Berry JD, Adler L, Koutalos Y, Kefalov VJ, and Cornwall MC (2016). Rhodopsin kinase and arrestin binding control the decay of photoactivated rhodopsin and dark adaptation of mouse rods. J. Gen. Physiol 148, 1–11. Available at: http://www.ncbi.nlm.nih.gov/pubmed/27353443 [Accessed February 26, 2018]. [PubMed: 27353443]

54. Nymark S, Frederiksen R, Woodruff ML, Cornwall MC, and Fain GL (2012). Bleaching of mouse rods: microspectrophotometry and suction-electrode recording. J. Physiol 590, 2353–2364. Available at: http://doi.wiley.com/10.1113/jphysiol.2012.228627. [PubMed: 22451436]

55. Govardovskii VI, Fyhrquist N, Reuter T, Kuzmin DG, and Donner K. (2000). In search of the visual pigment template. Vis. Neurosci 17, 509–528. Available at: http://www.scopus.com/inward/record.url?eid=2-s2.0-0033809503%7B&%7DpartnerID=40%7B&%7Dmd5=9bfa83b72058aa1b0d7094d6da1a6529. [PubMed: 11016572]

56. Wald G, and Brown PK (1953). The molar extinction of rhodopsin. J. Gen. Physiol, 189–200. [PubMed: 13109155]

57. Shichida Y, Imai H, Imamoto Y, Fukada Y, and Yoshizawa T. (1994). Is chicken green-sensitive cone visual pigment a rhodopsin-like pigment? A comparative study of the molecular properties between chicken green and rhodopsin. Biochemistry 33, 9040–9044. Available at: http://www.ncbi.nlm.nih.gov/pubmed/8049204 [Accessed October 9, 2019]. [PubMed: 8049204]

58. Irreverre F, Stone AL, Shichi H, and Lewis MS (1969). Biochemistry of visual pigments. I. Purification and properties of bovine rhodopsin. J. Biol. Chem 244, 529–36. Available at: http://www.ncbi.nlm.nih.gov/pubmed/5768853 [Accessed October 9, 2019]. [PubMed: 5768853]

59. Katz B, and Miledi R. (1972). The statistical nature of the acetycholine potential and its molecular components. J. Physiol 224, 665–99. Available at: http://www.ncbi.nlm.nih.gov/pubmed/5071933 [Accessed January 5, 2018]. [PubMed: 5071933]

HIGHLIGHTS

- Described single-cell biophysical method for analyzing dark cone transduction noise
- Dissected noise activity at each phototransduction step
- Dark apo-opsin activity is, surprisingly, even higher than dark pigment activity
- Apo-opsin content is high in L, less in M, and unresolvable in S cones

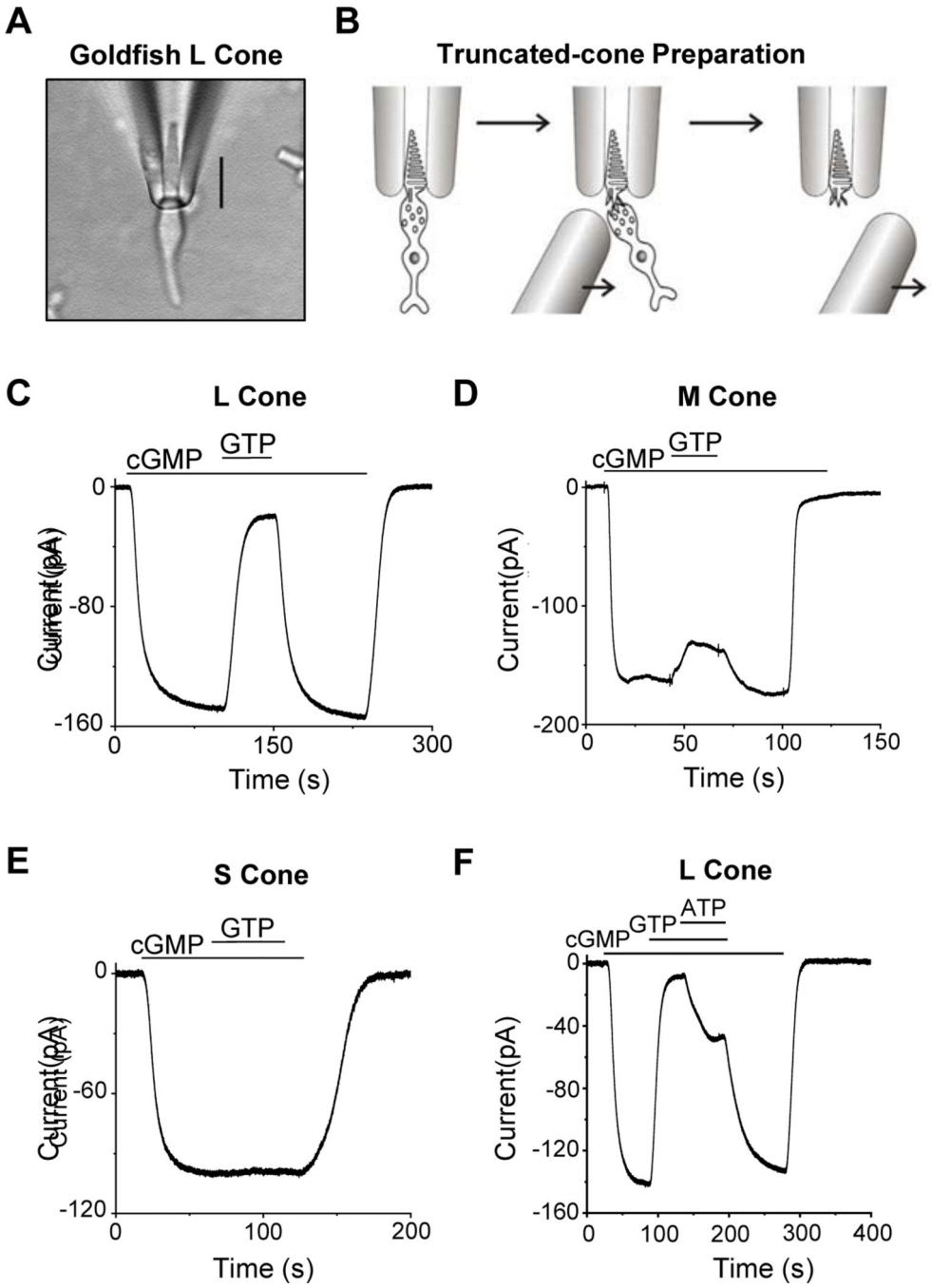

Figure 1. Truncated-cone recordings.

(*A*) Photomicrograph of a goldfish L cone with outer segment drawn into a suction-pipette electrode. (*B*) For truncated-cone recordings, a glass probe was used to separate the cone inner segment from the outer segment held in the pipette. After truncation, the intracellular compartment could be dialyzed through rapid solution changes. (*C*-*E*) Membrane current recorded from a truncated L (*C*), M (*D*) and S cone (*E*). The truncated cone was perfused continuously with a pseudo-intracellular solution, followed by addition of 500-μM cGMP which induced an inward current due to the opening of cyclic-nucleotide-gated (CNG)

channels. Next, 15-μM GTP was added into the perfusion solution, leading to a large current reduction in L cones (*C*), a small current reduction in M cones (*D*), but no detectable reduction in S cones (*E*). In each cone subtype, the effects of cGMP and GTP could be completely washed out. (*F*) ATP effect on dark GTP-dependent PDE activity. Addition of 1-mM ATP inhibited GTP-induced current reduction in an L cone, presumably by quenching pigment activity via pigment phosphorylation.

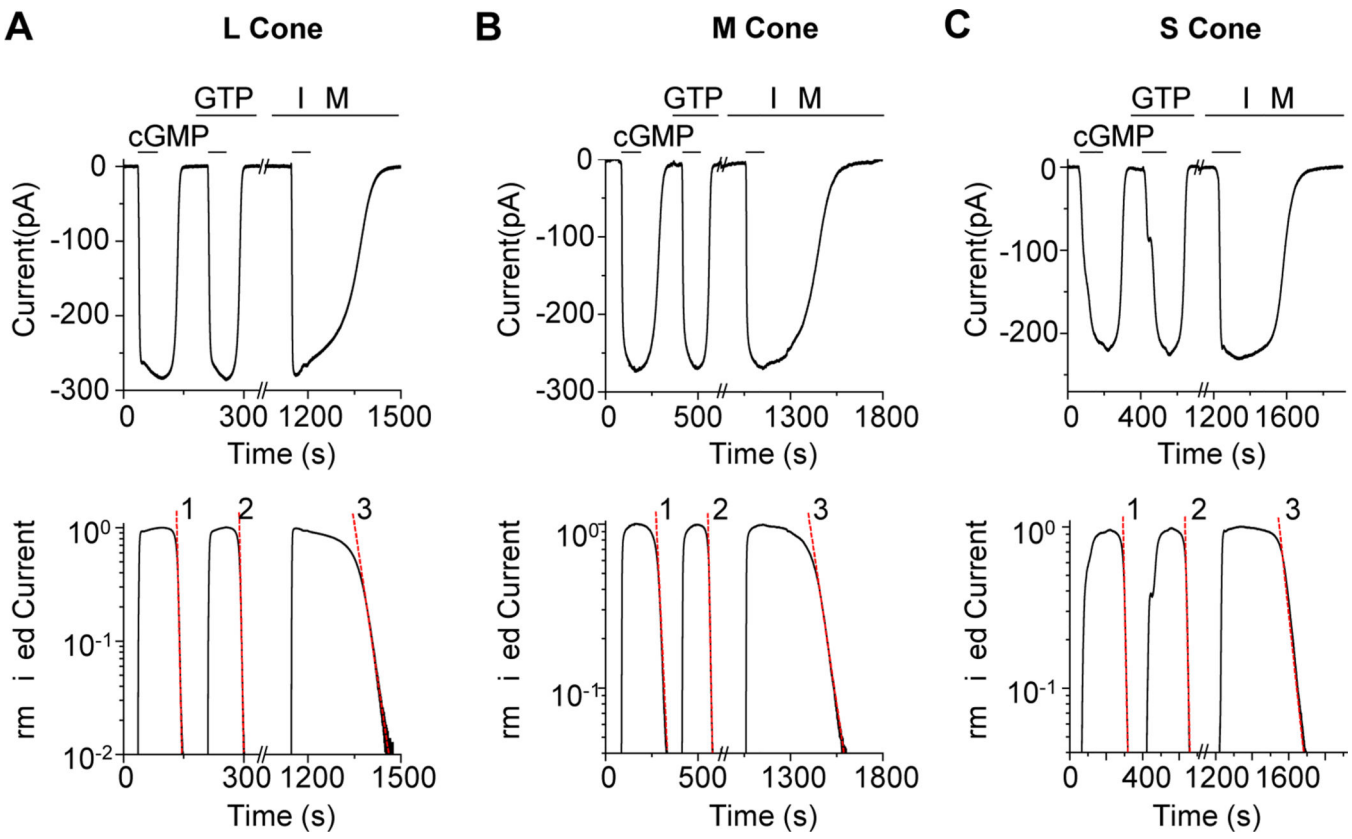

Figure 2. Quantification of dark PDE activity.

(*A*-*C*) *Top*, membrane current from a truncated L cone (*A*), M cone (*B*), and S cone (*C*) induced by 3-mM cGMP. In L and M cones, the current decay after bath cGMP removal was faster in the presence of 15-μM GTP, while in S cones, there was no detectable GTP-dependent PDE activity. In each cone subtype, the current decay was dramatically slowed down by addition of 1-mM IBMX, indicating substantial intrinsic PDE activity. (*A*-*C*) *Bottom*, semi-log plot showing single-exponential decline of membrane current (shown in Top panel) following each solution change. The semi-log slope values (dashed red line) of the exponential declines were used to calculate the intrinsic dark PDE activity, the spontaneous GTP-dependent PDE activity, and the cGMP diffusion coefficient for each cone subtype (see Text and Table S1).

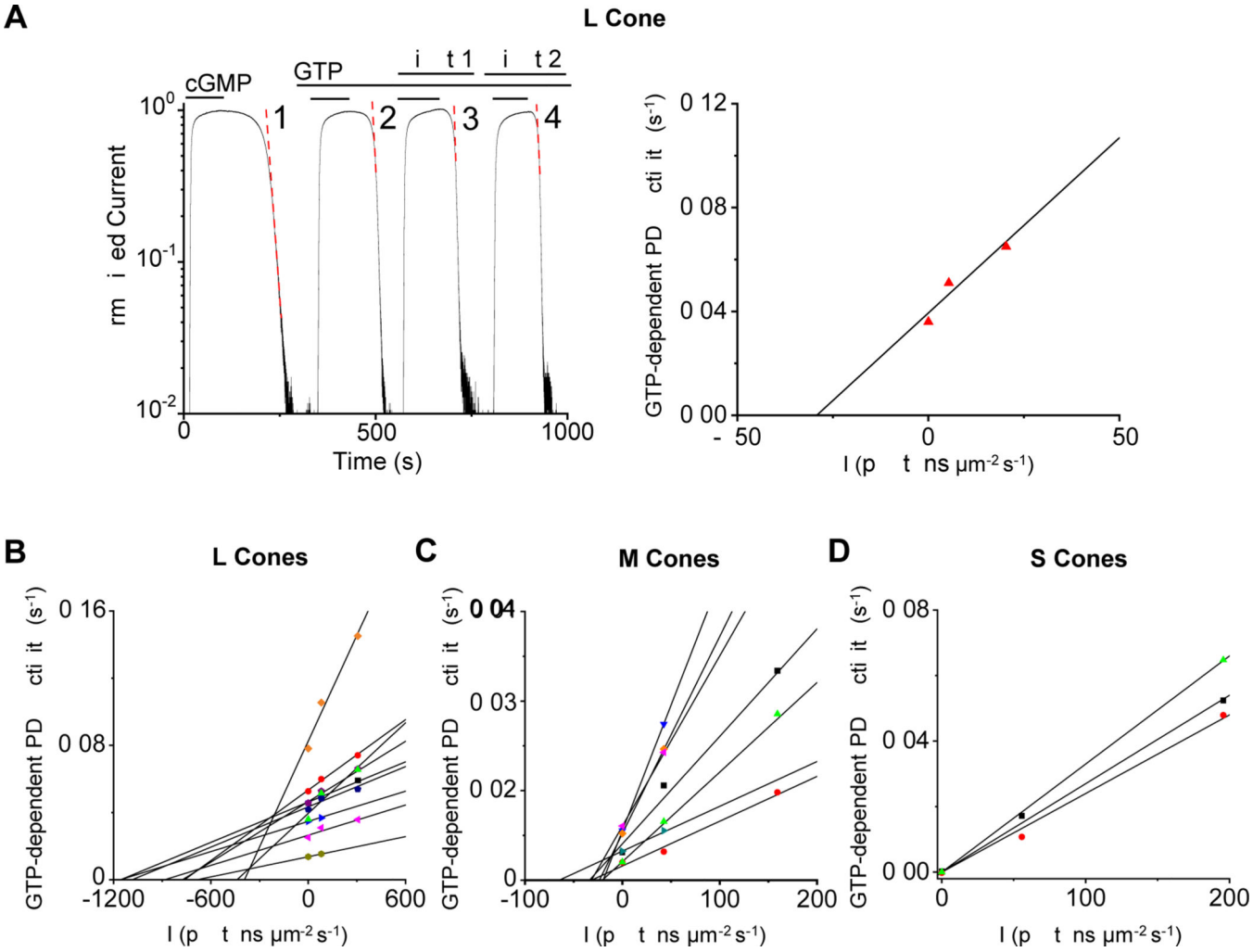

Figure 3. Equivalent dark light for dark PDE activities.

(*A*) *Left*, in a truncated L cone, GTP-independent and GTP-dependent (in the presence of 15-μM GTP) current decay (after brief exposure to 3-mM cGMP) was first measured in the dark. GTP-dependent current decay was then measured during exposure to steady light of 80 and 305 photons μm^{-2} s^{-1} at 620 nm, respectively. *Right*, the dark and light-induced GTP-dependent PDE activities are plotted against light intensities. A linear fit gives an abscissa intercept of −439 photons μm^{-2} s^{-1}, corresponding to the equivalent dark light of spontaneous GTP-dependent PDE activity in this particular L cone of 847 equivalent isomerizations s^{-1} (see Table S1 for effective collecting area). (*B-D*) Collected data from measuring the equivalent dark light of spontaneous GTP-dependent PDE activity in L cones (*B*), M cones (*C*), and S cones (*D*). Each set of symbols and linear fit represent a single cone. See also Table S1.

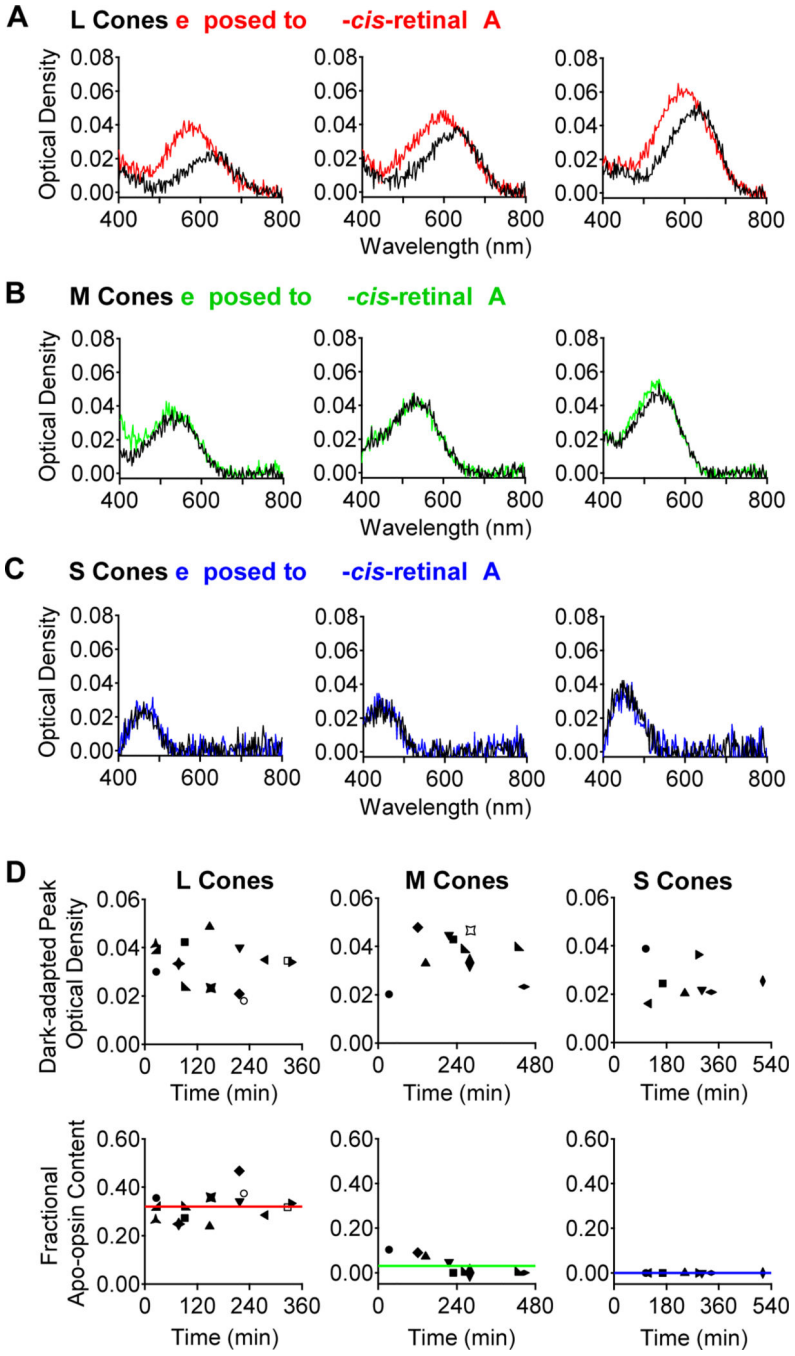

Figure 4. Apo-opsin content in dark-adapted goldfish cones.

(*A*) Optical-density measurements with microspectrophotometry on three individual dark-adapted L cones before (black) and after (red) exposure to 11-*cis*-retinal (A_1 chromophore). (*B, C*) Corresponding experiments on three dark-adapted M and S cones, respectively. The spectra represent absorbance in T-polarization for the L and M cones, and in T minus L polarization for the S cones. (*D*) Collected data. *Top,* Peak optical density and *Bottom,* calculated fractional apo-opsin content of dark-adapted L, M and S cones (see

STAR★METHODS). The mean apo-opsin content across all cells is indicated by solid red, green, or blue line for L, M, and S cones, respectively.

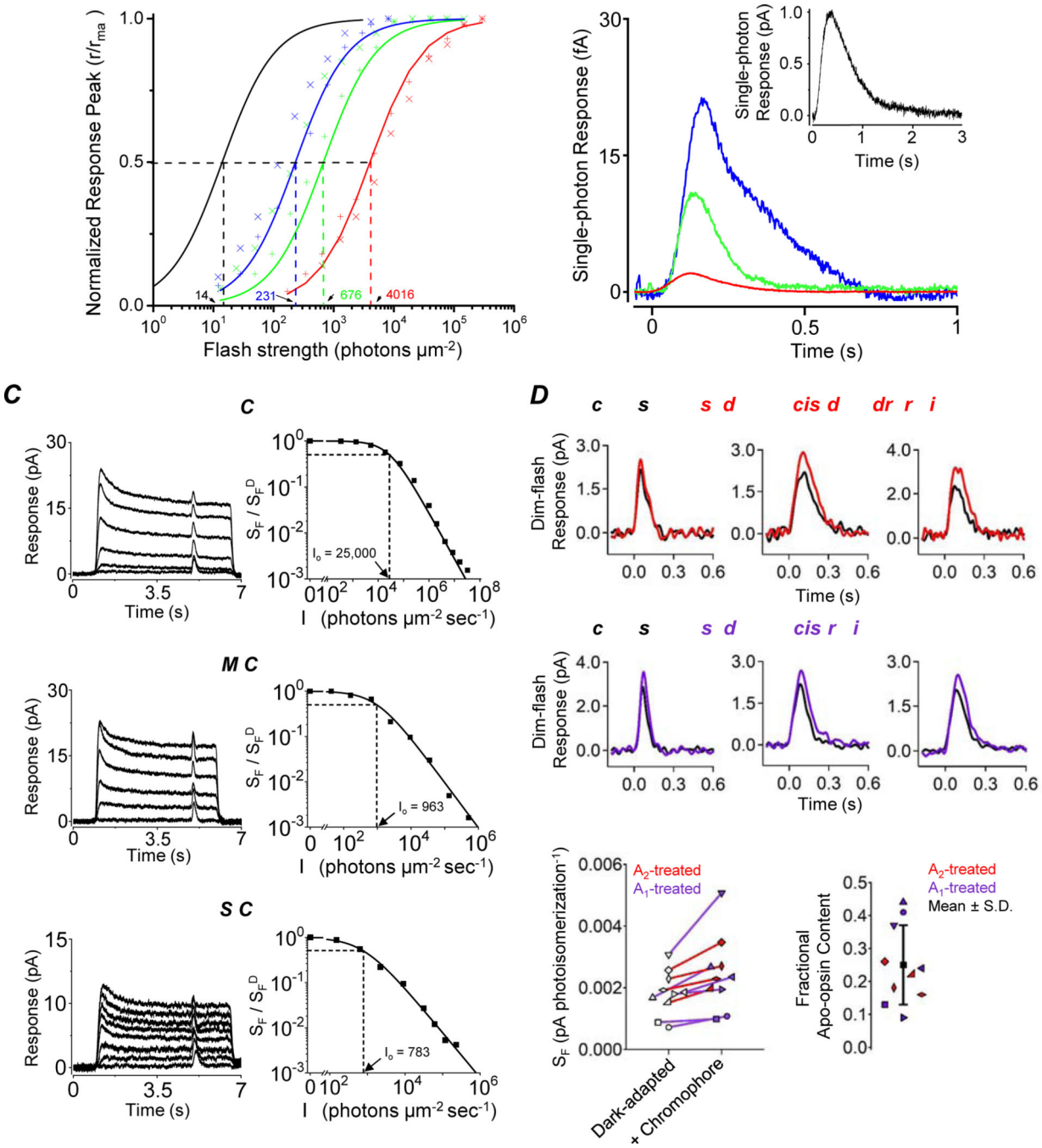

Figure 5. Response properties of goldfish L, M and S cones and the effect of exogenous chromophore.

(*A*) Intensity-response relations for L (red), M (green) and S cones (blue), and for rods (black). Each symbol represents a single cell. The curves are fits with $r/r_{max}=I_F/(\sigma+I_F)$ to the ensemble data for each photoreceptor subtype, where r and r_{max} are the transient-peak amplitude and maximal peak amplitude of flash responses, respectively; σ is the half-saturating flash intensity, and I_F is flash intensity. (*B*) Average single-photon responses of L (red), M (green) and S (blue) cones. *Inset*, average single-photon response of rods (black). Dim-flash response (averaged from 40–60 trials) is scaled to the average single-

photon response calculated from $r/(A_e \times I_F)$, where r is the transient-peak amplitude of ensemble average responses, A_e is the effective collecting area (Table S1), I_F is flash strength. (*C*) *Left,* Cone adaptation by steady light. Flash-responses elicited 5 sec after onset of steady background light of different intensities. *Right*, Normalized incremental-flash sensitivity as a function of background light intensity. *Top*, *middle*, and *bottom* panels are data from an L, M, and S cone, respectively. Curves are fits with the Weber-Fechner Law I_o is a constant corresponding to a light intensity that reduces sensitivity by one-half. (*D-G*) The physiological effect of regenerating apo-opsin in dark-adapted cones. (*D*) Dim-flash responses of three dark-adapted L cones before (black) and after 4-min exposure to A_2 chromophore (10-μM 11-*cis*-dehydroretinal, red). (*E*) Corresponding experiments with A_1 chromophore (10-μM 11-*cis*-retinal, purple). (*F*) Collected data showing the effect on sensitivity for each cell exposed to A_2 (red) or A_1 (purple) chromophore. (*G*) Calculated apo-opsin content based on the increased sensitivity shown in (*F*) and after adjusting for the different light-absorption characteristics of A_1 versus A_2 chromophore (see STAR★METHODS). See also Table S1.

KEY RESOURCES TABLE

REAGENT or RESOURCE	SOURCE	IDENTIFIER
Chemicals, Peptides, and Recombinant Proteins		
Lipid-free Bovine Serum Albumin	Sigma-Aldrich	A6003
11-*cis*-retinal	National Eye Institute, Laboratory of Masahiro Kono, Medical University of South Carolina	
11-*cis*-dehydroretinal	Laboratory of Masahiro Kono, Medical University of South Carolina	
Experimental Models: Organisms/Strains		
Goldfish	Ozark Fisheries	Pond Comets
Software and Algorithms		
pClamp 10	Molecular Devices	10.5.2.6
Igor Pro	WaveMetrics	6.11
OriginPro	OriginLab Corporation	2020